# Investigation of Current Density Distribution Model for Barb-plate ESP

GUO Yinliang[1], XIANG Xiaodong[2], CHEN Baozhi[1]
(1 College of Resources & Civil Engineering, Northeastern University, Shenyang 110004, PR China
2 Hubei key laboratory for efficient utilization and agglomeration of metallurgic mineral resources, Wuhan University of Science and Technology, Wuhan 430081, PR China)

**Abstract:** In order to satisfy Gaussian electric flux theorem, current distribution at the plane of barb-plate electrostatic precipitator (ESP) must follow a certain specified distribution function. It is proved that, in this paper, the current distribution at the plane of barb-plate ESP is *t*-distribution with 4 degree of freedom by variable analysis on Warburg's Law. According to the characteristics of the current distribution, a more applicable calculation formula is derived by using the total current at the plate electrode. The values predicted by our *t*-distribution model are in sound agreement with the experimental data presented by other researchers.

**Keywords:** barb-plate electrode, ESP, current density, *t*-distribution

## 1 INTRODUCTION

The barb-plate electrostatic precipitators have been widely used in industrial air pollution control because of their good performances, such as better voltage-current characteristics, stronger corona discharge, higher drift velocity of charged particles, etc[1]. Current density at the ground plate is an important factor which influences the performance of barb-plate ESP. High corona current is beneficial for particulate collection in ESP since more ions can be produced to increase particle charging rates to saturation or limiting values[2]. However, high corona current, at same time, leads to high current density at the ground plate. As we know that the electric field in the dust layer is given by

$$E = j \cdot \rho$$

in which $j$ is the current density and $\rho$ is the dust layer resistivity. In the case of high resistivity dust, if the strength of the electric field in the dust layer exceeds electrical breakdown value, the back corona appears. The back corona could possibly lead to the collection efficiency of ESP decreasing significantly. If the current density distribution on the collection plate is relatively uniform, the back corona can be weakened significantly. In the industrial electrostatics precipitator applications, the maximum current density value at the electrical breakdown point may be decreased to 1/10 of the theoretical calculation[3] due to the non-uniformity of the current density distribution at the plate electrode. It is important, therefore, to discuss the current density distribution in order to optimize the arrangement of the electrodes in barb-plate ESP.

Many researchers had studied the current density distributions at the ground electrode in barb-plate ESP[4,5,6]. However, there are two problems that are not well solved today. One is that the current density distribution models they proposed do not satisfy Gaussian electric flux theorem. Another is that their models are not convenient for practical use since the current density at the plate directly under the barb electrode is difficult to be calculated. Then, a current density distribution formula, which is not only strict in theory, but also applicable in practice, is needed to be developed.

## 2 BRIEF REVIEWS ON CURRENT DENSITY DISTRIBUTIONS OF BARB-PLATE ESP

A well-known empirical expression for the current density distributions on the plate beneath a barb electrode, see Fig. 1, was presented by Warburg in 1899, namely, the famous Warburg's law

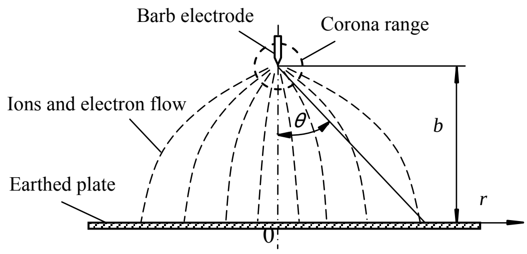


**Fig. 1** Scheme of the barb-plate corona discharge

$$\begin{aligned} j(\theta) &= j(0)\cos^m \theta, \quad \theta \le 60° \\ j(\theta) &= 0, \quad \theta > 60° \end{aligned} \tag{1}$$

where $j(0)$ is the current density directly under the barb electrode, $\theta$ is the semi-cone angle from the centerline, and *m* is a parameter that was determined to be 4.82 for positive coronas and 4.65 for negative coronas by curve fitting.

The value of *m* in Eq. (1) had been interested by some researchers[7,8]. Although Warburg's experiment used gaps between the barb and ground plate in the centimeter range, Eq. (1) is able to descript the current density distributions at the plate electrode accurately for gaps from a few millimeters to several meters[9,10]. Some new formulae for current density distributions were presented based on Warburg's law. One of the analytic expressions was developed by Sigmond[4], using the unipolar charge-drift approach, that is

$$j(\theta) = j(0)(1 + \tan\theta)^{-3/2} \tag{2}$$

Sigmond concluded that the results of Eq. (2) were very close to those of Warburg's law and agreed with the experimental values presented by Kondo and Goldman by comparison analysis. Jones[5] has also shown mathematically that Sigmond's expression is the same as Warburg's law (with $m$=5). By assuming that the ions flight along the elliptical path, Jones[6] improved Warburg's expression

$$j(\theta) = j(0)\cos^5\theta \cdot f(\theta) \tag{3}$$

where, $f(\theta) = 1/\sqrt{1-\frac{3}{4}\sin^4\theta - \frac{1}{4}\sin^6\theta} \approx 1$ .

However, the current density distribution expressions mentioned above are just the modifications of Warburg's law. All above formulae, actually, do not satisfy the Gaussian electric flux theorem.

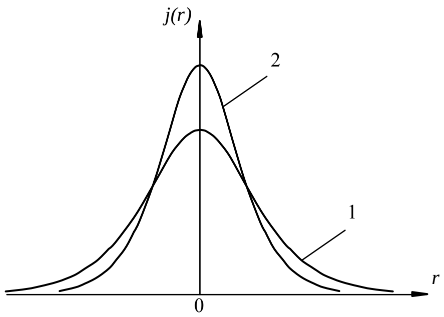


**Fig. 2** Scheme of current density distribution at the ground plate

The characteristic of the current density distributions at the ground plate of barb-plate ESP is that the value of the current density reaches the peak value directly under the barb, and decreases gradually to both sides till to 0 if $r \to \infty$, as shown in Fig. 2. According to Gaussian electric flux theorem, the electric flux at any plane between the barb and plate must be equal to the electric flux at the ground plate. That is, the area under the curve-2 equals the area under the curve-1. In order to agree with the characteristics presented above and satisfy Gaussian electric flux theorem, current distributions at the plane of barb-plate ESP must follow a certain specific distribution function. Two distribution functions cloud meet the conditions above. They are normal distribution and $t$-distribution.

## 3 CURRENT DENSITY DISTRIBUTION FUNCTION OF BARB-PLATE ESP

First, assuming that the current density distributions at the ground plate follows a normal distribution

$$j(r) = \frac{A}{2\pi\sigma^2}\exp(-\frac{r^2}{2\sigma^2}) \tag{4}$$

where $\sigma$ is the Variance and $A$ is a constant need to be determined. Integrating Eq. (4) over the whole ground plate area (from $r=0$ to $r\to\infty$), it gives $A$=$I$. In which $I$ is the total current. Then, Eq. (4) can be written as

$$j(r) = \frac{I}{2\pi\sigma^2}\exp(-\frac{r^2}{2\sigma^2}) \tag{5}$$

Now we need to test whether the current density distribution has normal distribution or not. According to the experimental results by Goldman et. al.[11], when the total current $I$=150 μA, $j(0)$=71 μA·cm$^{-2}$, thus, $\sigma$ is determined to be 0.58 by Eq. (5). and the results calculated from the Eq. (5) are compared with the experimental results by Goldman et. al., as shown in Fig. 3. Greater deviations can be seen in Fig.3 between the normal model and experimental values, while the values calculated form Warburg's law fit the experimental data better. It is signified that the assumption of the normal model of the current density distributions is not reasonable. Then, the $t$-distribution model has to be discussed next.

It is concluded from the research carried out by Sigmond[4] and Jones[6] that $m$=5 in Warburg's law is acceptable. Then, Eq. (1) can be written as

$$j(\theta) = j(0)\cos^5\theta \tag{6}$$

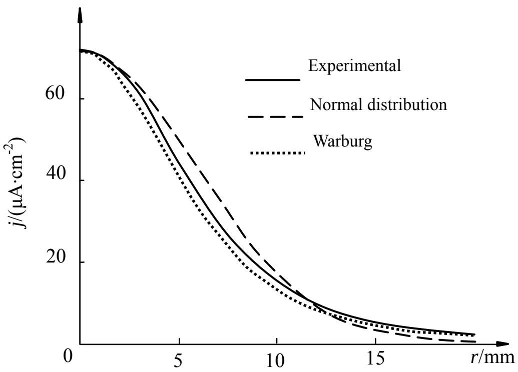


**Fig. 3** Current density distribution comparison of measured value, normal model, as well as Warburg's law

Because

$$\cos\theta = \frac{b}{\sqrt{b^2+r^2}} \tag{7}$$

So, the Warburg's law can now be written

$$j(r) = j(0)[1+(\frac{r}{b})^2]^{-5/2}. \tag{8}$$

The density function of the $t$-distribution is

$$h(t) = \frac{\Gamma[(n+1)/2)]}{\sqrt{n\pi}\Gamma(n/2)}(1+\frac{t^2}{n})^{-(n+1)/2} \tag{9}$$

where $n$ is the degree of freedom, $t$ is the independent variable.

When $n$=4, Eq. (9) becomes

$$h(t) = \frac{3}{8}(1+\frac{t^2}{4})^{-5/2} \tag{10}$$

Let $r = bt/2$, then

$$t = 2r/b\ . \tag{11}$$

Substituting Eq. (11) into Eq. (10), gives

$$h(2r/b) = \frac{3}{8}[1+\frac{(2r/b)^2}{4}]^{-5/2} = \frac{3}{8}[1+(\frac{r}{b})^2]^{-5/2} \tag{12}$$

Comparing Eq. (8) with Eq. (12), it is evident that the variable part $[1+(\frac{r}{b})^2]^{-5/2}$ in Eq. (12) is just the same as the factor $\cos^5\theta$ in Eq. (8). So the current density distributions at the ground plate of the barb-plate ESP have a *t*-distribution with independent variable $t = 2r/b$ with 4 degrees of freedom. The expression is

$$j(r) = \xi h(2r/b) \tag{13}$$

In which $\xi$ is the coefficient need to be determined.

## 4 DETERMINATION OF THE COEFFICIENT $\xi$

According to the characteristics of the current distributions, the value of the integration of Eq. (13) over the whole ground plate must be equal to the total current *I*, as shown in Fig. 4. That is

$$I = \int_0^{2\pi}\int_0^{+\infty} j(r) r dr d\beta .$$

$$= \int_0^{2\pi}\int_0^{+\infty} \xi \frac{3}{8}[1+(r/b)^2]^{-5/2} r dr d\beta \quad \text{b} \tag{14}$$

Solving Eq. (14), gives

$$\xi = \frac{4I}{\pi b^2} \tag{15}$$

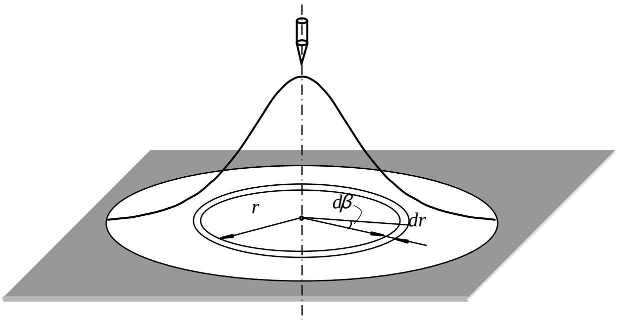


**Fig. 4** Scheme of current distribution at the ground plate

Substituting Eq. (12) and Eq. (15) into Eq. (13), we have

$$j(r) = \frac{3I}{2\pi b^2}[1+(r/b)^2)]^{-5/2} \tag{16}$$

It is easily proved that the value of integrating Eq. (16) over the whole plate electrode is always equal to the total current *I*. Therefore, the *t*-distribution model for the current density distributions at the collecting plate of the barb-plate ESP always satisfies Gaussian electric flux theorem.

## 5 TEST FOR THE T-DISTRIBUTION OF CURRENT DENSITY

The current density distributions have been measured in air by many researchers. The pencil-shaped discharge electrode was used by Goldman et. al.[11], and the gap separation *b* was 10 mm for the experiments. The total current *I* was determined by controlling the applied voltage. Three cases were chosen to be compared with the value calculated by using *t*-distribution model, corresponding to typical values of large, medium and small overall current, namely 150 μA, 80 μA and 30 μA, as shown in Fig. 5. It can be seen form Fig. 5 that the values predicted by *t*-distribution model are very close to the experimental results. The lower the total current is, the closer the calculation values are to the measurement values. When the total current *I* is 30 μA, the theoretical curve and the experimental curve are almost coincident. The values calculated by Warburg's law are also shown in Fig. 5 for comparison. It is obvious that the calculation results of Warburg's law are also close to the experimental values. However, Warburg's law is an empirical curve-fitting model, and it doesn't satisfy Gaussian electric flux theorem.

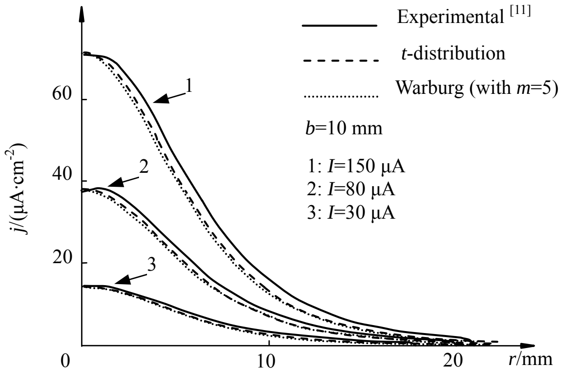


**Fig. 5** Comparison of current density distribution between *t*-distribution model and the experimental value presented by Goldman et. al.[11]. (calculation values of Warburg's law are also shown in this figure)

The *t*-distribution model has also a good agreement with the experimental results presented by McKinney et. al.[12], shown in Fig. 6. In the measurement of McKinney, the barb with the tip curvature radius is 0.073 mm, and the gap separation *b* is 7.0 7cm. The total current *I* is 169 μA when 50 kV DC voltage is applied. Even though the values calculated by *t*-distribution model do not quite fit the experimental values presented by McKinney et. al. at the center area of collection electrode (the difference is about 0.1 $\mu A \cdot cm^{-2}$), the relative deviation is only about 6%, as seen from Fig. 6. The theoretical values are more close to the experimental results as the distance form the centerline of *r* increasing. When the distance *r* is greater than 35 mm, the theoretical values are almost exactly equal to the experimental data.

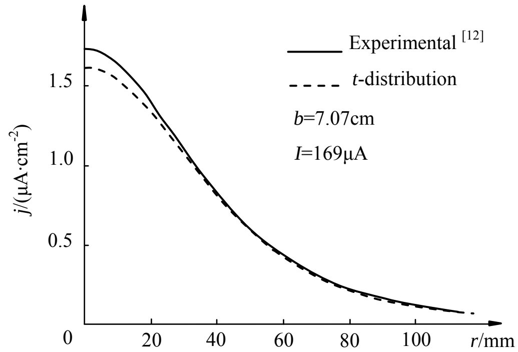


**Fig. 6** The comparison of current density distribution from the *t*-distribution model and experimental value presented by McKinney et. al.

## 6 CONCLUSIONS

(1) The current density distributions at the plate electrode of the Single barb-plate electrode system have a *t*-distribution with 4 degrees of freedom. This model does not only satisfy Gaussian electric flux theorem, but also has very good agreement with the experimental results.

(2) The prominent merit of the model presented in this paper is that the current density distributions at the ground plate can be determined easily by using the total current *I* and the gap separation *b*. The model is more applicable than the expressions proposed before because *I* and *b* can both be measured directly. This model is also very useful for optimizing the arrangement of the electrodes in barb-plate ESP.

## ACKNOWLEDGEMENTS

This work was supported under National Natural Science Foundation of China (Contract 50778139) and Project of Wuhan Science and Technology Bureau (Agreement 200760423161).

## REFERENCES

1. A. Jaworek, A. Krupa and T.Czech. Modern electrostatic devices and methods for exhaust gas cleaning: A brief review [J]. J. Electrostatics, 2007, 65: 133-155.
2. J.R. McDonald, A.H. Dean. Electrostatic Precipitator Manual [M]. New York: Noyes, 1982.
3. S. Oglesby, G.B. Nichols. Electrostatic Precipitation [M]. New York: Marcel Dekker, Inc., 1983.
4. R.S. Sigmond. Simple approximate treatment of unipolar space-charge-dominated coronas: the Warburg law and the saturation current [J]. J. Appl. Phys, 1982, 53 (2): 891-898.
5. J.E. Jones, A.M. Cohen. Chebyshev Comparisons of current laws for point-plane DC coronae in air [J]. J. Electrostatics, 1997, 39: 111-128.
6. J.E. Jones. A theoretical explanation of the laws of Warburg and Sigmond[J]. Proc. Roy. Soc. London A. 1997, 453: 10331052.
7. A. Goldman, E.O. Selim and R.T. Waters. Current distribution in the negative corona discharge in air[C]. In Proceedings of the Fifth GD, Liverpool, 1978: 87-91.
8. K.J. McLean, I.A. Ansari. Calculation of the rod-plane voltage/current characteristics using the saturated current density equation and Warburg's law [J]. IEE Proc. 1987, 134 (10, Part A): 784-788.
9. A. Goldman , M. Goldman and J.E. Jones. On the behaviour of the planar current distribution in the pulseless regime of negative DC point-plane coronas in air[C]. In Proceedings of the Tenth GD, Swansea, 1992: 270-273.
10. T.E. Allibone, J.C. Saunderson. Corona at very high direct voltages, Corona in rod/plane gaps [C]. In Proceedings of ISH89, New Orleans, 1989：22.02.
11. A. Goldman, M. Goldman and J.E. Jones, et. al. Current distributions on the plane for point-plane negative coronas in air, nitrogen and oxygen [C]. In Proceedings of the Ninth GD, Venice, 1988: 197-200.
12. P.J. McKinney, J.H. Davidson, and D.M. Leone. Current distributions for barbed plate-to-plane coronas [J]. IEEE Trans. Industry Applications, 1992, vol 28, no.6: 1424-1431.